Journal Name

RSCPublishing

ARTICLE

Halogen-Bonding in a New Family of tris(haloanilato)metallate(III) Magnetic Molecular Building Blocks

Cite this: DOI: 10.1039/x0xx00000x

Received 00th January 2012,
Accepted 00th January 2012

DOI: 10.1039/x0xx00000x

www.rsc.org/

Matteo Atzori,[†] Flavia Artizzu,[†] Elisa Sessini,[†] Luciano Marchiò,[‡] Danilo Loche,[†] Angela Serpe,[†] Paola Deplano,[†] Giorgio Concas,[§] Flavia Pop,[ǁ] Narcis Avarvari,[ǁ] and Maria Laura Mercuri[†,*]

Electronic Supplementary Information

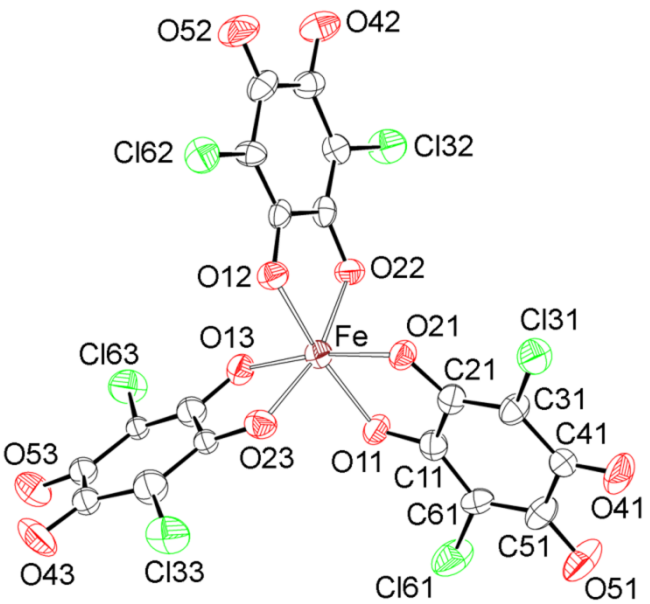

Figure S1 Ortep drawing for **2b** with thermal ellipsoids at the 30% probability level. $(Ph_4)P^+$ cations and crystallization water molecule were omitted for clarity.

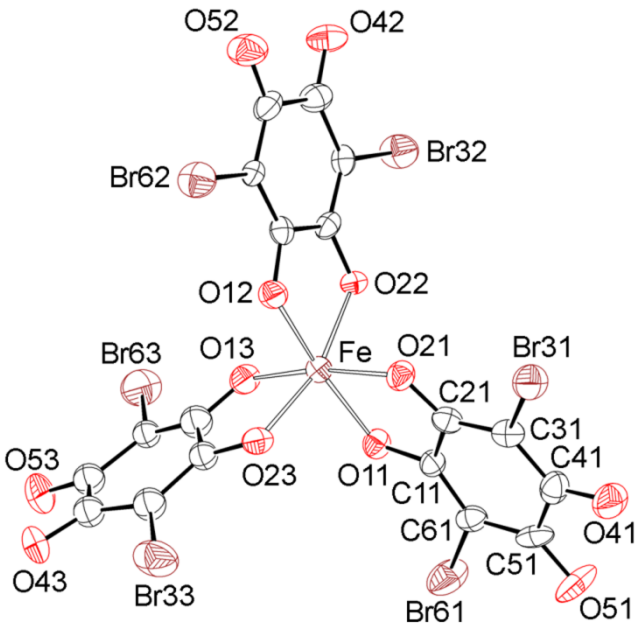

Figure S2 Ortep drawing for **4b** with thermal ellipsoids at the 30% probability level. $(Ph_4)P^+$ cations and crystallization water molecule were omitted for clarity.

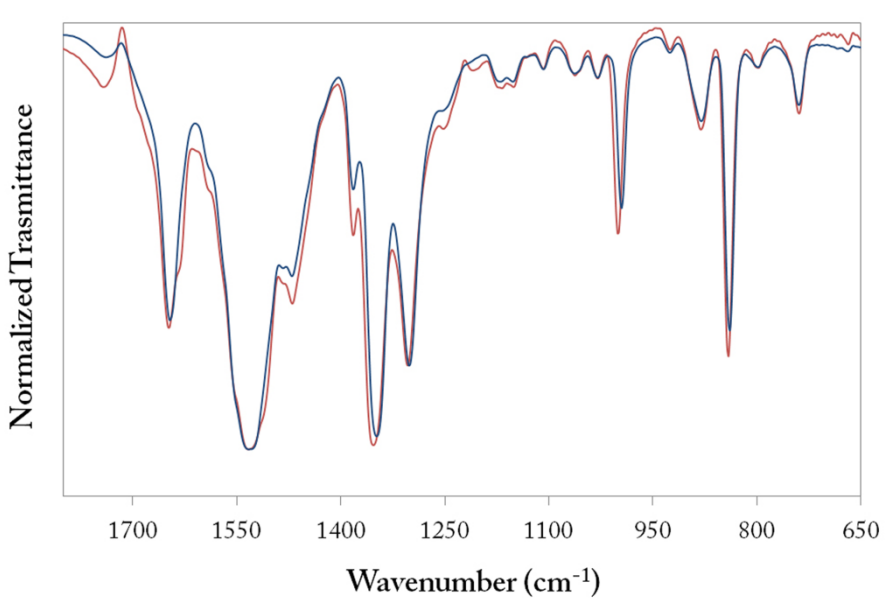

Figure S3 FT-IR spectra (1800-650 cm^{-1}) for **1a** (red line) and **2a** (blue line).

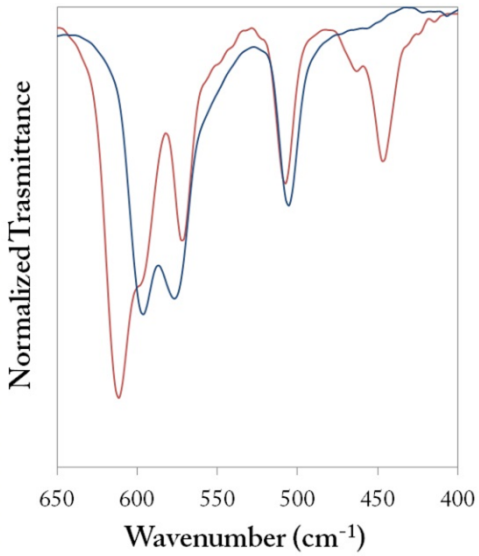

Figure S4 FT-IR spectra (650-400 cm^{-1}) for **1a** (red line) and **2a** (blue line).

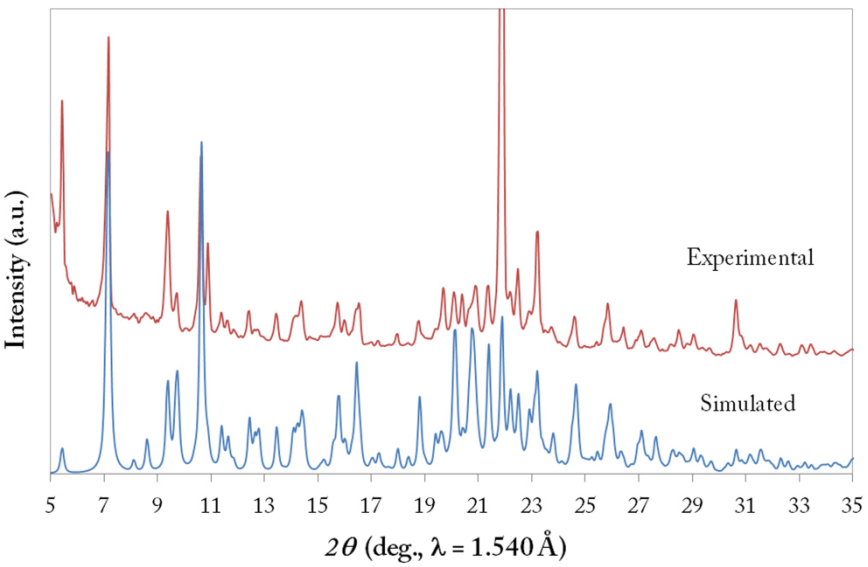

Figure S5 Comparison between experimental (red line) and simulated (blue line) PXRD patterns (5-35°, 2θ) for **2b**.

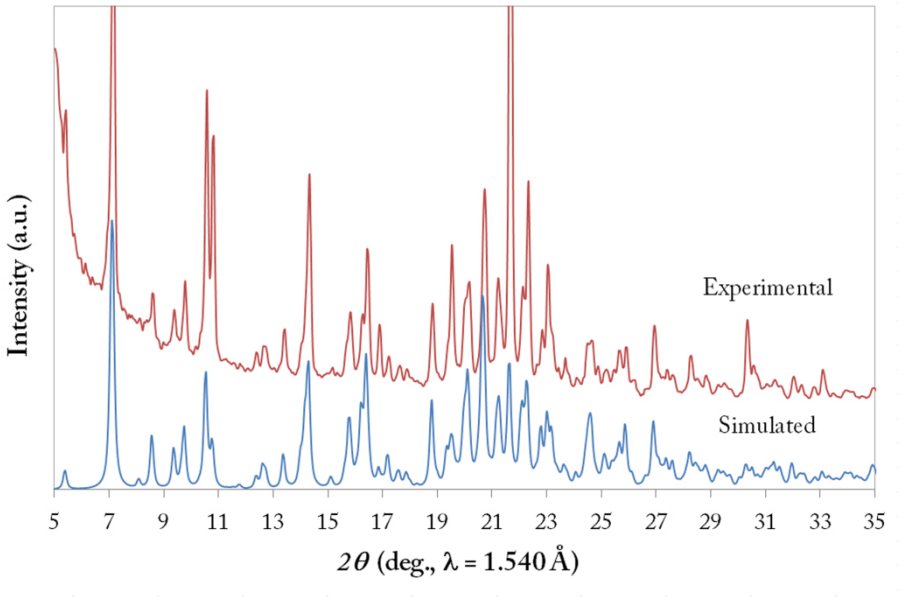

Figure S6 Comparison between experimental (red line) and simulated (blue line) PXRD patterns (5-35°, *2θ*) for **4b**.

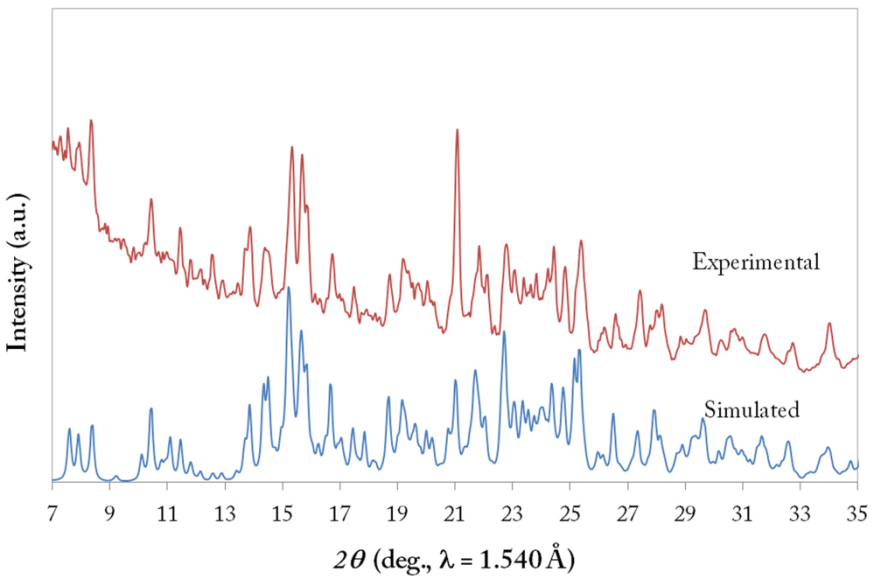

Figure S7 Comparison between experimental (red line) and simulated (blue line) PXRD patterns (5-35°, *2θ*) for **6b**.

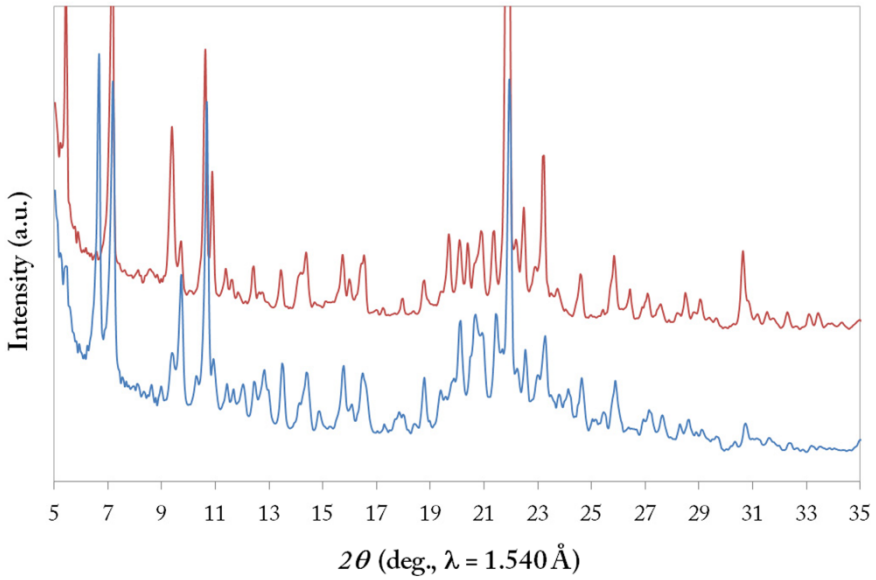

Figure S8 Comparison between experimental PXRD patterns (5-35°, *2θ*) for **1b** (blue line) and **2b** (red line).

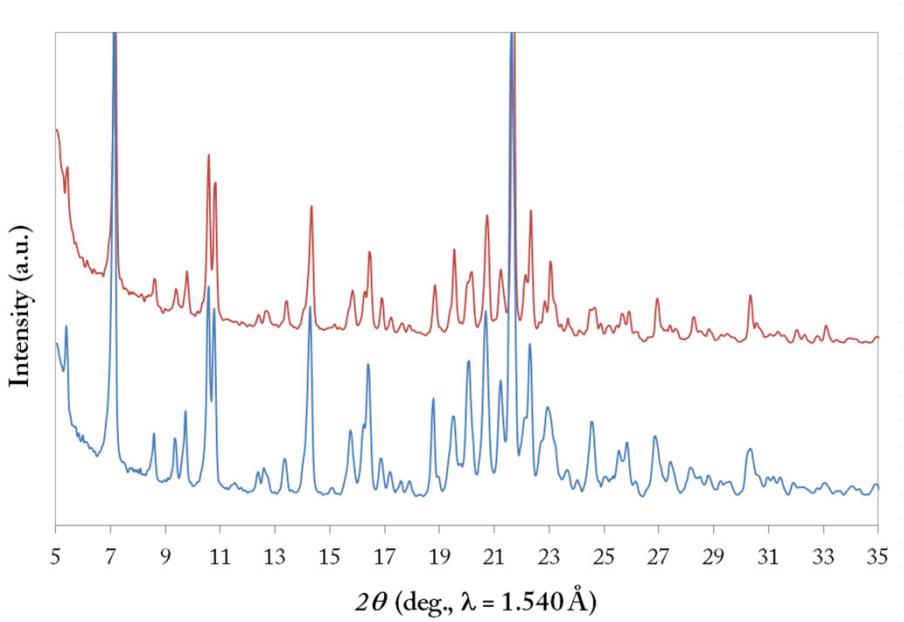

Figure S9 Comparison between experimental PXRD patterns (5-35°, *2θ*) for **3b** (blue line) and **4b** (red line).

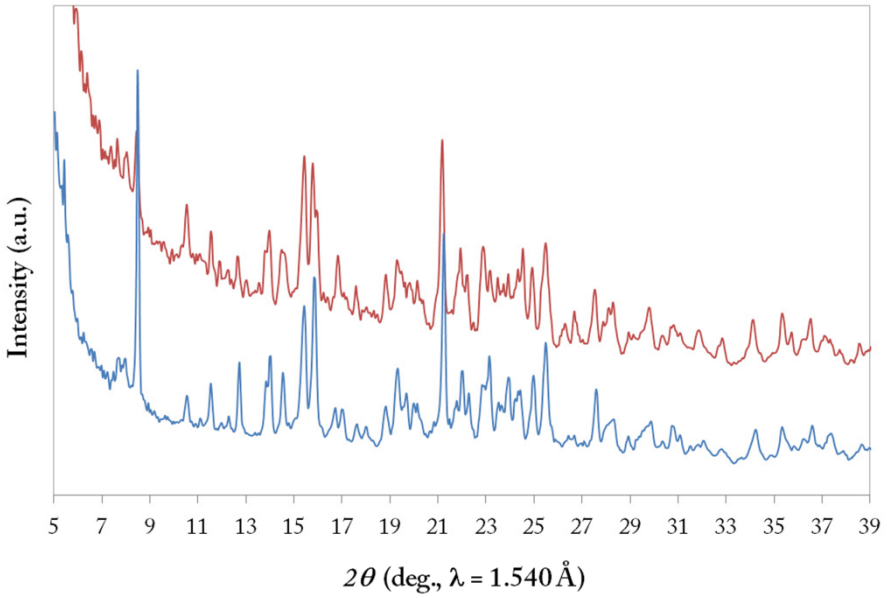

Figure S10 Comparison between experimental PXRD patterns (5-39°, 2θ) for **5b** (blue line) and **6b** (red line).

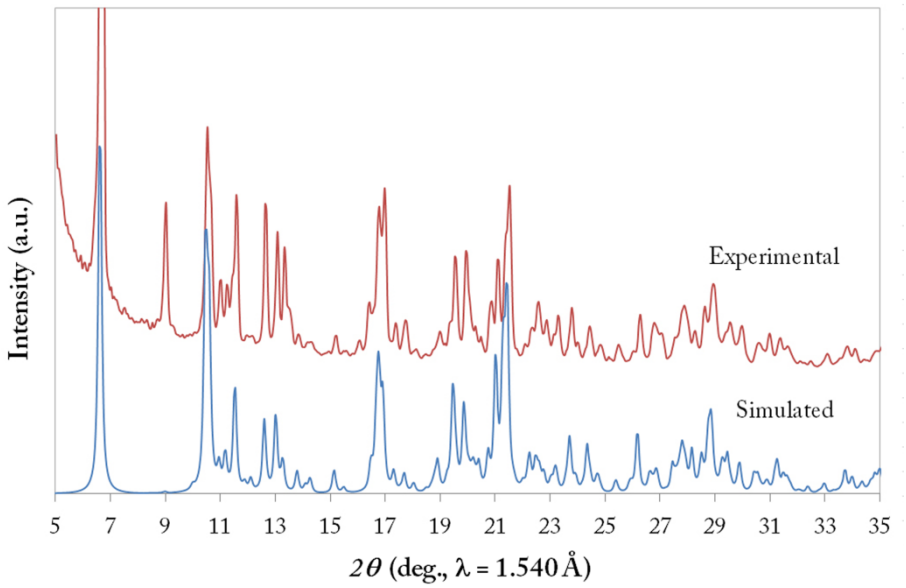

Figure S11 Comparison between experimental (red line) and simulated (blue line) PXRD patterns (5-35°, 2θ) for **1c**.

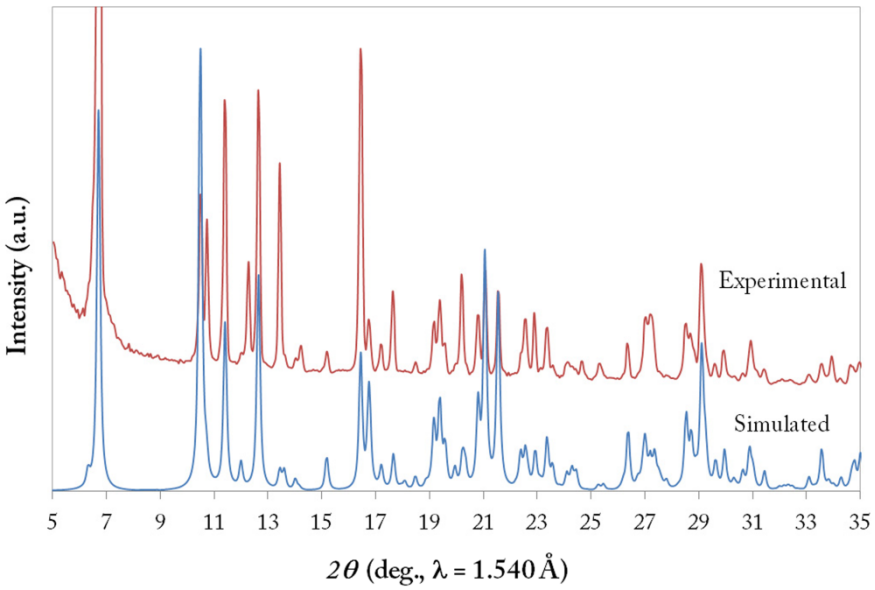

Figure S12 Comparison between experimental (red line) and simulated (blue line) PXRD patterns (5-35°, *2θ*) for **2c**.

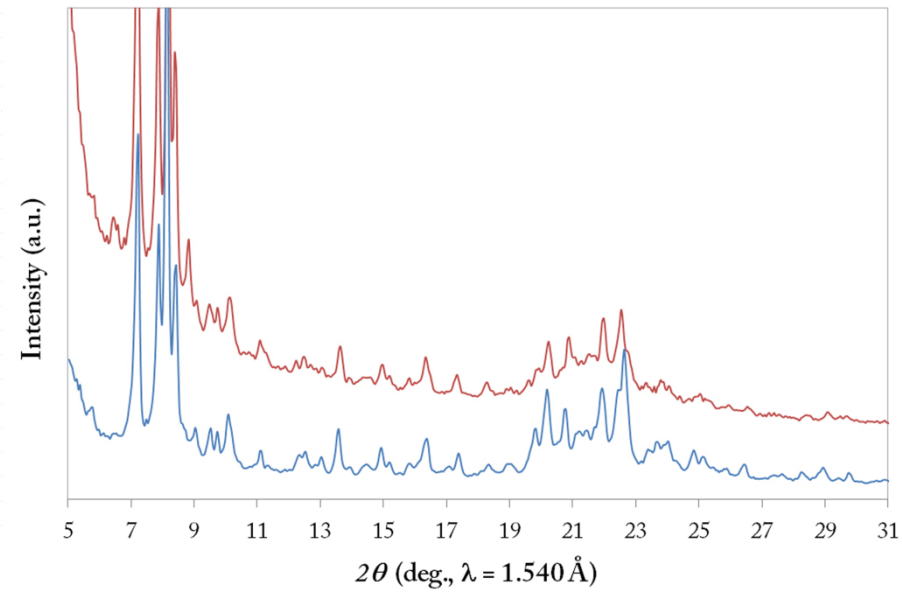

Figure S13 Comparison between experimental PXRD patterns (5-31°, *2θ*) for **1a** (blue line) and **2a** (red line).

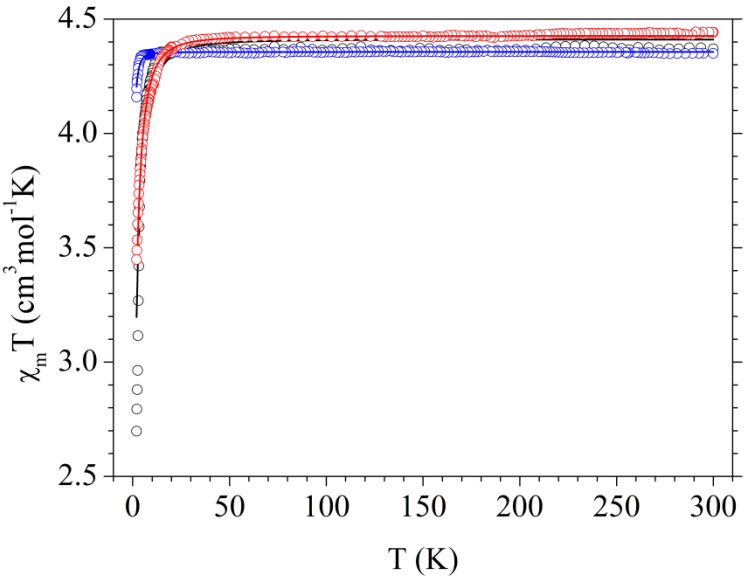

Figure S14 Thermal variation of the $\chi_m T$ product for **2a** (black circles), **2b** (red circles), and **2c** (blue circles). Solid lines are the best fit of the model (see text).

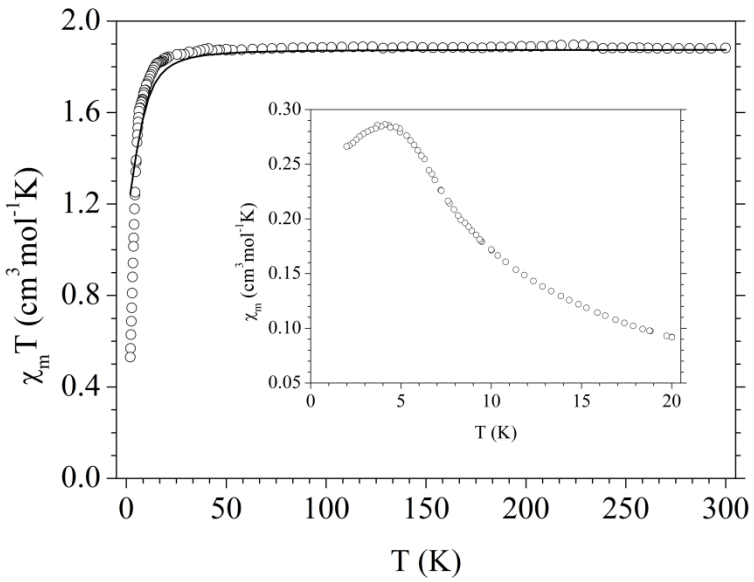

Figure S15 Thermal variation of the $\chi_m T$ product for **5a**. Solid line is the best fit of the model which takes into account the zero field splitting (see text). The inset shows the maximum of the susceptibility.

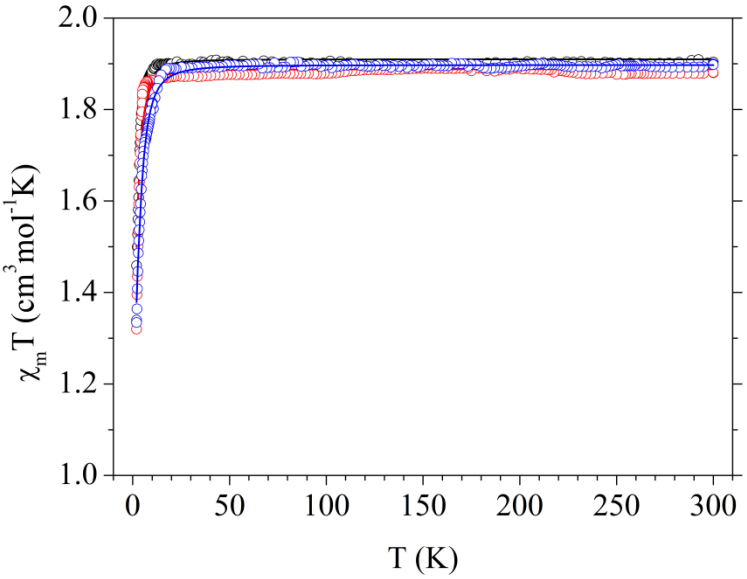

Figure S16 Thermal variation of the $\chi_m T$ product for **1a** (black circles), **1b** (red circles), and **1c** (blue circles). Solid lines are the best fit of the model (see text).

Table S1 Selected vibrational frequencies for $[Cr(Cl_2An)_3]^{3-}$ (**1**), $[Fe(Cl_2An)_3]^{3-}$ (**2**), $[Cr(Br_2An)_3]^{3-}$ (**3**), $[Fe(Br_2An)_3]^{3-}$ (**4**), and $[Cr(I_2An)_3]^{3-}$ (**5**), and $[Fe(I_2An)_3]^{3-}$ (**6**).

Vibrational mode	**1**	**2**	**3**	**4**	**5**	**6**
ν(C=O)	1650	1647	1639	1640	1630	1630
ν(C=C) + ν(C-O)	1530	1530	1521	1521	1513	1515
ν(C-O) + ν(C-C)	1353	1349	1343	1337	1330	1326
ν(C-O) + ν(C-C) + δ(C-X)	1000	995	988	978	968	962
δ(C=O) + δ(C-O) + ν(C-X)	841	839	808	803	779	781
ρ_w(C-X)	572	574	558	560	548	551

Table S2 Cyclic Voltammetry data for compounds **1-6**.

Oxidation Potential	**1**	**2**	**3**	**4**	**5**	**6**
1st Oxidation Peak	+1.23	+1.23	+1.33	+1.31	+1.32	+1.30
2nd Oxidation Peak	-	+1.37	-	+1.43	-	+1.66